2006

Predicting the percent live cover of corals: An in situ remote sensing approach

Deepak R. Mishra
University of Nebraska-Lincoln

Sunil Narumalani
University of Nebraska - Lincoln, snarumalani1@unl.edu

Ronald Bahl
University of Nebraska - Lincoln

D. Rundquist
University of Nebraska-Lincoln, drundquist1@unl.edu

Merlin P. Lawson
University of Nebraska-Lincoln, mlawson1@unl.edu

Predicting the percent live cover of corals: An in situ remote sensing approach

Deepak R. Mishra,[1] Sunil Narumalani,[1] Ronald Bahl,[1] Donald Rundquist,[1] and Merlin Lawson[1,2]

Received 3 November 2005; revised 27 January 2006; accepted 31 January 2006; published 18 March 2006.

[1] Percent reflectance of corals is perhaps the most important remotely sensed data that can be related to their biophysical properties. Because most of the biophysical variables of corals (i.e., pigment content, live cover and algal overgrowth) are related to their reflectance spectra, the analysis and inversion of the spectra may provide an account of these variables. Our research was aimed at determining the relationship between the percent live cover and reflectance of corals. Two wavelength bands (405–425 nm, and 590–600 nm) were identified to establish the relationship. A linear relationship was observed, which showed higher correlation ($R^2 = 0.886$) at 405–425 nm when compared to 590–600 nm ($R^2 = 0.602$). Validation methods revealed that 405–425 nm wavelength range provided a better relationship than 590–600 nm in predicting percent live cover of corals. **Citation:** Mishra, D. R., S. Narumalani, R. Bahl, D. Rundquist, and M. Lawson (2006), Predicting the percent live cover of corals: An in situ remote sensing approach, *Geophys. Res. Lett.*, *33*, L06603, doi:10.1029/2005GL025056.

1. Introduction

[2] Environmental stress on coral reefs can result from natural and human influences. Natural causes include global rise in temperature and sea level [*Pittock*, 1999], increased frequency of El Niño Southern Oscillation (ENSO) events [*Timmermann et al.*, 1999], tropical cyclones [*Knutson et al.*, 1998], and increased concentrations of atmospheric CO_2 [*Kleypas et al.*, 1999], while human activities include coastal development, destructive fishing, marine pollution, runoff from deforestation, and industrial/agricultural discharge. The net effect of most disturbances is a reduction in the percent cover of living coral over time, and with remote sensing techniques these temporal variations can be used to detect any shifts in the "health" of the corals [*English et al.*, 1997].

[3] Roatan Island, located in the western portion of the Caribbean Sea is the largest of the Bay Islands of Honduras, and over the past century, damaging hurricanes have occurred, with the most serious ones being Hurricanes "Fifi" (1974) and "Mitch" (1998) [*Kuta and Richardson*, 1996]. In general, there is a decreasing pattern of live coral cover off Roatan, from west to east, accompanied by increasing amount of algal cover along the same transect [*Fonseca*, 1997]. In a 1997 coral survey, the Sandy Bay/West End Marine Reserve reef system of Roatan Island had 24.6–52.8% live coral, and 18.4–56.6% algal cover [*Fonseca*, 1997]. These facts have raised alarm in various sectors, including recreational, tourism, and political communities. There is an emerging consensus to map out the spatial distribution of live corals around Roatan Island so that protection, preservation, and monitoring measures can be implemented.

[4] The objective of our study investigates possible relationships between percent live cover (PLC) of corals and their reflectance (R) observed from in situ hyperspectral remote sensing measurements. It was hypothesized that since most of the biophysical variables (pigment content, live cover, and algal overgrowth) of corals are related to their light reflectance spectra, the analysis and inversion of the spectra may provide an account of these variables. Because reflectance spectra of corals is the only common property that relate in situ-airborne-spaceborne remote sensing observations, our research can also be applied to airborne and spaceborne data which would aid in mapping PLC of corals in a cost effective way.

[5] In situ spectral measurements of reef biota suggest that the major functional forms (species-level identification) of corals were distinguishable when measured using the narrow spectral bands (1–2 nm) of a hand-held spectro-radiometer [*Holden and LeDrew*, 1999]. A major problem involved with such in situ sensing is the light attenuation in the water column overlaying the substrate, which significantly affects the signal [*Maritorena*, 1996]. In our research, water column corrections were applied to the hyperspectral reflectance spectra of corals. An Adjustable Buoyancy Device (ABD) was devised and used as a profiler inside the water column acquiring upwelling radiance (L_u) and downwelling irradiance (E_d) at different depths. This sampling methodology allowed comparison of R values of the same substrate at different depths and different PLC.

2. Methodology

2.1. System Design

[6] Data were acquired in April 2005 along the northwestern coast of Roatan Island. Two independent in situ data sets were collected at different locations; one for model calibration and one for model validation. Our experimental design allowed systematic measurement of R values immediately above (10 cm) the corals and at different depths up to just below the air-water interface. The ABD served as the mounting platform for all sensors to measure

[1]Center for Advanced Land Management Information Technologies, School of Natural Resources, University of Nebraska, Lincoln, Nebraska, USA.

[2]Department of Geosciences, University of Nebraska, Lincoln, Nebraska, USA.

0094-8276/06/2005GL025056

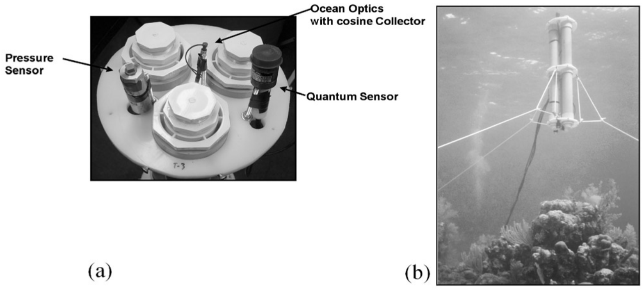

Figure 1. (a) Top part of the Adjustable Buoyancy Device (ABD) showing different sensors; (b) ABD in action under water.

L_u and E_d while simultaneously capturing digital images of the area of interest (AOI) at varying depths within the water column. The sensors mounted on the ABD included Ocean Optics USB 2000 hyperspectral radiometers, quantum sensor, pressure sensor, and a digital camera (Figure 1a). The L_u and E_d were then used to calculate R values while the digital images were used to determine PLC. The ABD had a system of pulleys and ropes that allowed three divers to secure the device vertically within the water column above the area of interest (AOI). The ABD (Figure 1b) was designed to be vertically buoyant within the water column with three divers serving as anchor points and controlling it via pulleys. In addition, the ropes allowed the divers to adjust the height of the ABD above the coral surface to facilitate scanning at different depths.

2.2. Coral Percent Reflectance (R)

[7] The R values of corals at various depths were calculated in two ways: (a) without incorporating water column effects, and (b) removing the water column effect.

$$\textbf{a)}\quad R = \frac{L_u}{E_d} \times 100 \tag{1}$$

L_u (W m^{-2} sr^{-1}) and E_d (W m^{-2}) were measured from downward and upward looking hyperspectral sensors respectively.

$$\textbf{b)}\quad R = \frac{L_{ou}}{E_{od}} \times 100 \tag{2}$$

L_{ou} (W m^{-2} sr^{-1}) and E_{od} (W m^{-2}) are upwelling radiance and downwelling irradiance respectively, without the presence of water column. L_{ou} and E_{od} can be derived by applying Beer's law as:

$$L_u = L_{ou}\exp(-K_u dz) \Rightarrow L_{ou} = \frac{L_u}{\exp(-K_u dz)} \tag{3}$$

$$E_d = E_{od}\exp(-K_d dz) \Rightarrow E_{od} = \frac{E_d}{\exp(-K_d dz)} \tag{4}$$

where,

dz = depth interval in m between successive measurements
K_u = attenuation coefficient in m^{-1} for L_u
K_d = attenuation coefficient in m^{-1} for E_d

2.3. Derivation of K_u and K_d

[8] Beer's law states that intensity of light decreases exponentially as a function of depth in the water column and is described as:

$$E = E_0 e^{(-Kdz)} \tag{5}$$

where,

E = irradiance at a given depth
E_0 = irradiance at the surface
K = attenuation coefficient

In our experiment, L_u and E_d measurements were taken at several incremental depths therefore; Beer's law for L_u can be modified to:

$$L_u(z_m) = L_{ou}(z_1)e^{-\int_{z_1}^{z_m} K_u dz} \tag{6}$$

where,

$$L_{ou}(z_1) = L_u \text{ at depth } z_1$$

$$L_u(z_m) = L_u \text{ at depth } z_m$$

To simplify equation (6), the natural logarithm was derived as follows:

$$-\int_{z_1}^{z_m} K_u dz = \ln[L_u(z_m)] - \ln[L_{ou}(z_1)] \tag{7}$$

Furthermore, assuming K_u being constant for all dz (the assumption was made after analyzing the K_u values for different dz; the results showed very little difference in the K_u value), equation (7) can be modified as:

$$-K_u(z_m - z_1) = \ln\left[\frac{L_u(z_m)}{L_{ou}(z_1)}\right] \tag{8}$$

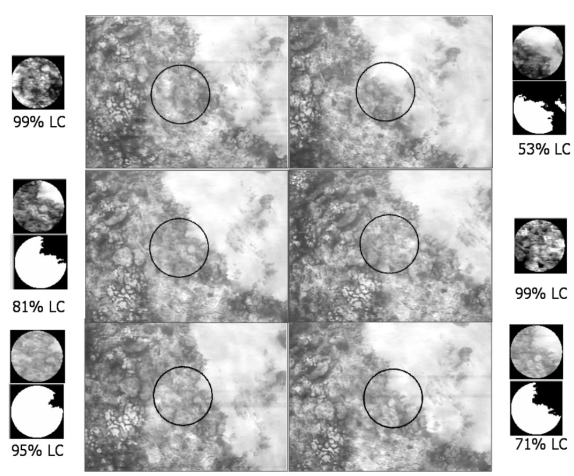

Figure 2. Photographs of the coral cover taken from the camera. The small black circle within each photograph indicates the IFOV of the hyperspectral radiometer. Areas within these circles were used to calculate the PLC as shown on the sides.

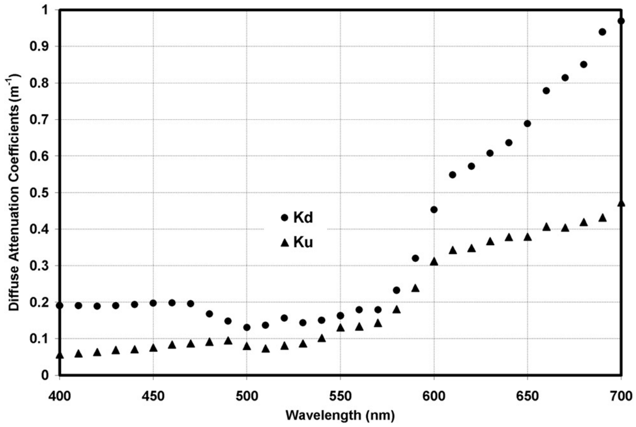

Figure 3. Upwelling and downwelling diffuse attenuation coefficients.

Equation (8) corresponds to the equation of a straight line passing through origin (y = mx). In a plot of ln $\left[\frac{L_u(z_m)}{L_{ou}(z_1)}\right]$ versus $(z_m - z_1)$, the local slope provides the K_u. Similarly, K_d was also derived.

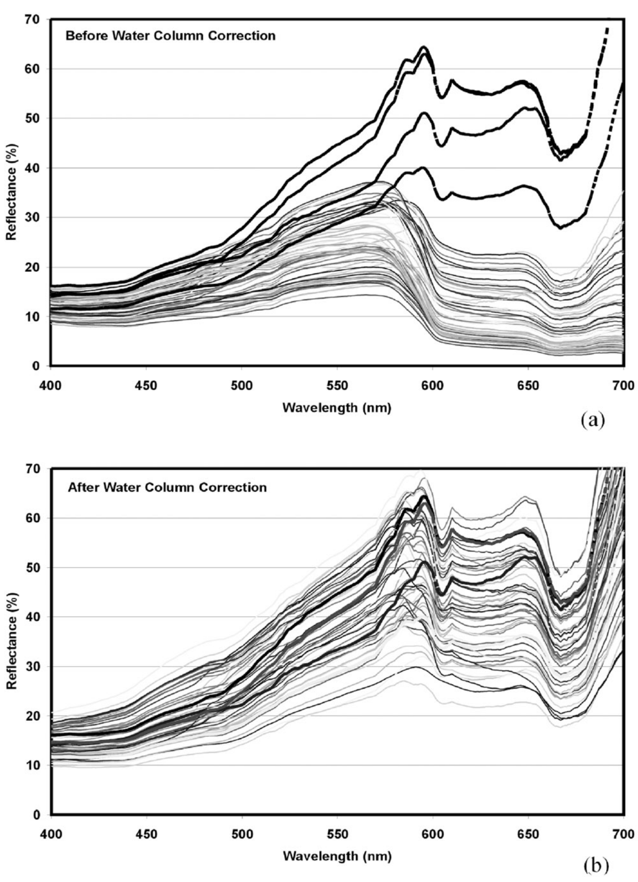

Figure 4. Reflectance (R) of corals with varying PLC (a) before water column correction; (b) after the water column correction. The thick black dotted lines in each graph indicate the in situ coral reflectance spectra.

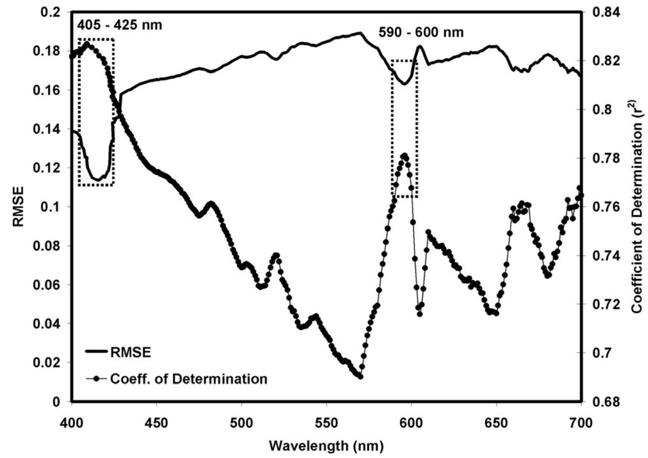

Figure 5. *RMSE* and r^2 of PLC estimation. The wavelength ranges in the rectangular were chosen for further analysis.

2.4. Percent Live Cover (PLC)

[9] A total of 23 digital images (12 for model calibration and 11 for model validation) were acquired during the experiment at two locations. Instantaneous Fields of View (IFOVs) of the digital camera and radiometer were 95° and 25° respectively. The common AOIs were clipped out from the digital images by using the distance of the sensors from the target. Seed pixels of live corals (versus sand) were visually interpreted and image processing tools such as region growth were used to expand those areas. Still photographs from a video camera were also used in the interpretation process. The parameters were adjusted to only incorporate pixels that represented live coral. PLC for each image was calculated by dividing the number of live coral pixels by the total number of pixels in the image. Photographs of coral benthos taken by the digital camera and the IFOV subtended by the hyperspectral sensor (black circles within each photograph) are shown in Figure 2. The areas within the circle were used to calculate the PLC (shown in the small rectangles along the sides of the photographs in Figure 2). It is important to remember that this process is subject to visual interpretation and therefore, unintended bias may have occurred.

3. Results

[10] In Case 1 waters such as Roatan, the absorption of the red wavelengths by water itself was higher because of the low concentrations of suspended particles. As light becomes diffused in the water column, the red absorption increases, which in turn raises the K values exponentially - specifically from 560 nm onward (Figure 3). However, the magnitude of K in case of L_u was smaller than E_d. In general, the blue region showed higher K than the green region (500 –550 nm) because chlorophyll present in the coral phytoplankton cells absorb the blue wavelengths. R values of coral, before and after the water column removal, showed the remarkable effect of red light attenuation (Figures 4a and 4b). The thick dotted lines in the graphs are the R values of coral from in situ (<10 cm) measurements determined by spectral absorption and

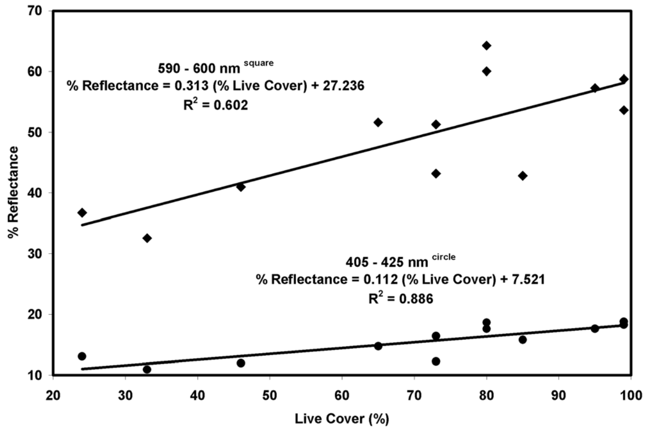

Figure 6. Model calibration plot showing the relationship between *R* and PLC at select wavelength ranges.

fluorescence properties of multiple pigments residing at various locations in a coral colony, including the zooxanthellae, as well as the ectodermal and endodermal host tissues [*Dove et al.*, 1995]. Variability in each of these pigment sources contributed to the complexity in shape and the magnitude of *R* values. Typical reflectance spectra of coral (dotted lines) exhibited relatively low values between 400 to 500 nm, higher between 550 and 650 nm, a narrow chlorophyll absorption feature at 675 nm, and a rapid increase from 680 nm onward. The magnitude of *R* values ranged from ~10% at blue to ~90% in the red wavelengths. In our case the *R* values showed a triple-peaked pattern which is characterized by low reflectance between 400–500 nm and by high reflectance (i.e., local maxima) near 575, 650, and 675 nm (Figure 4b). These reflectance variabilities, caused by absorption and fluorescence of coral-host pigments, were absent in the spectra before water column correction (Figure 4a). Light reflected from the coral benthos was basically mixed with contributions from the water column (absorption, scattering), specifically in the red wavelengths (Figure 4a). After the water column effects were removed, the same set of spectra showed the absorption and reflectance details of coral features, and comparable magnitudes of *R* values to the in situ data.

[11] The focus of this research was to examine if there was any relationship between a wavelength band and PLC of corals. This relationship (if any), can only be established with representative spectra produced after the water column correction. To find the spectral bands where *R* was sensitive to PLC, coefficient of determination (r^2) and root mean square error (*RMSE*) of estimation between *R* and PLC were analyzed (Figure 5). Two wavelength bandwidths were identified (405–425 nm, and 590–600nm) where the r^2 were relatively high, i.e., 0.82 and 0.78 and the *RMSE* were low, i.e., 0.11 and 0.16 respectively. Those ranges were used to establish a relationship between reflectance and PLC. Model calibration was performed by using the samples collected during the experiment at the first location. A linear relationship was found between *R* and PLC at the two wavelength bands, however, it was more prominent in the case of 405–425 nm (R^2 = 0.886) when compared to 590–600 nm range (R^2 = 0.602) (Figure 6). At 590–600 nm there was a greater deviation of the observations from the trend line, with the intercept being 27.236 (as compared to 7.521 for 405–425 nm) which may be due to the higher reflectance (pigment scattering) of brown and blue healthy corals.

[12] PLC of the next set of samples was predicted by inverting the calibration equation. Validation of the model revealed that the 405–425 nm range is a better predictor because the reflectance spectra of coral appear to be affected by only one factor, i.e., chlorophyll absorption. Conversely, in the 590–600 nm range reflectance is affected by both pigmentation and structure of the coral. In relating *R* with PLC, only spectral variation due to pigment concentration was considered, while structure was not. Residuals reveal no clear pattern of over- or under-estimation (Figure 7, inset). However, they show that estimation error increases at higher PLC (>70%).

4. Discussion

[13] Researchers have had some success in calculating PLC from airborne remote sensing [*Mumby et al.*, 2004] using clustering and derivative analyses. One of the main factors affecting consistent results was the effect of the water column on the reflectance properties of corals. There is always a temptation to interpret readily observable variations in remotely sensed color of water as a direct indicator of water quality, or benthic type, without correcting for water column effects. Initially, remote sensing specialists attempted to develop strategies to monitor the extent and vitality of coral reefs, often by assuming the effects of the water column above to be horizontally and vertically homogeneous [*Holden and LeDrew*, 2001]. More recently, investigators have determined these assumptions of homogeneity to be overly simplistic. Our research provides indications that further processing (i.e., water column correction) to airborne or space-borne remotely sensed images is necessary for coral live cover mapping. Better results may also be expected in predicting the PLC by applying other correction factors such as changing sun illumination, wave action, wave

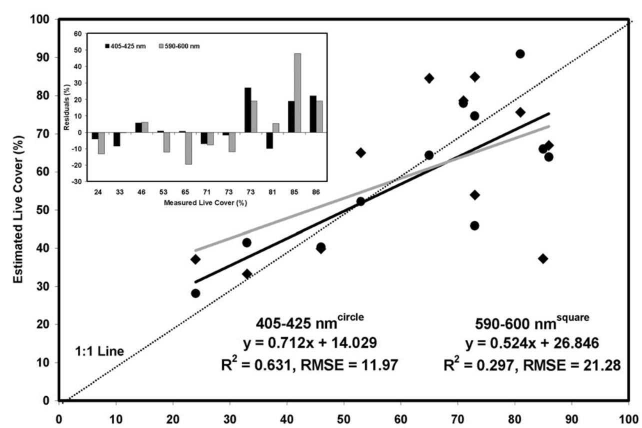

Figure 7. Model validation depicting measured vs. estimated PLC and histogram plot of residuals (inset).

focusing, and instrument self-shadow on the reflectance spectra acquired by ABD.

[14] **Acknowledgments.** The authors thank the field crew of the Center for Advanced Land Management Information Technologies (CALMIT), University of Nebraska-Lincoln (UNL), and staff at the Roatan Institute for Marine Science for their data collection efforts. The funding for the work was provided by CALMIT, the University Research Council, and the School of Natural Resources, UNL.

References

Dove, S. G., M. Takabayashi, and O. Hoegh-Guldberg (1995), Isolation and partial characterization of the pink and blue pigments of Pocilloporid and Acroporid corals, *Biol Bull.*, *189*, 288–297.

English, S., C. Wilkinson, and V. Baker (1997), *Survey Manual for Tropical Marine Resources*, 2nd ed., 390 pp., Aust. Inst. of Mar. Sci., Townsville, Queensl., Australia.

Fonseca, A. C. (1997), Rapid assessment of the Sandy Bay/West End Marine Reserve (RMSW) Reef System, limits and zonification, Management Priorities and Recommended Reef Monitoring Plan, 9 pp., Roatán Inst. of Mar. Sci., Roatán, Honduras.

Holden, H., and E. LeDrew (1999), Hyperspectral identification of coral reef features, *Int. J. Remote Sens.*, *20*, 2545–2563.

Holden, H., and E. LeDrew (2001), The effects of the water column on hyperspectral reflectance of submerged coral reef features, *Bull. Mar. Sci.*, *69*, 685–699.

Kleypas, J. A., R. W. Buddemeier, D. Archer, J. P. Gattuso, G. Langdon, and B. Opdyke (1999), Geochemical consequences of increased atmospheric carbon dioxide on coral reefs, *Science*, *284*, 118–120.

Knutson, T. R., R. E. Tuleya, and Y. Kurihara (1998), Simulated increase of hurricane intensities in a CO_2-warmed climate, *Science*, *279*(5353), 1018–1020.

Kuta, K., and L. L. Richardson (1996), Abundance and distribution of blackband disease on coral reefs in the northern Florida Keys, *Coral Reefs*, *15*, 219–223.

Maritorena, S. (1996), Remote sensing of the water attenuation in coral reefs: A case study in French Polynesia, *Int. J. Remote Sens.*, *17*, 155–166.

Mumby, P. J., J. D. Hedley, J. R. M. Chisholm, C. D. Clark, and J. Jaubert (2004), The cover of living and dead corals using airborne remote sensing, *Coral Reefs*, *23*, 171–183.

Pittock, B. A. (1999), Coral reefs and environmental change: Adaptation to what?, *Am. Zool.*, *39*, 10–29.

Timmermann, A., M. Latif, A. Bacher, J. Oberhuber, and E. Roeckner (1999), Increased El Nino frequency in a climate model forced by future greenhouse warming, *Nature*, *398*, 694–696.

R. Bahl, M. Lawson, D. R. Mishra, S. Narumalani, and D. Rundquist, Center for Advanced Land Management Information Technologies, School of Natural Resources, University of Nebraska, Lincoln, NE 68588, USA. (dmishra@calmit.unl.edu)